CHAPTER 3

SYSTEM DESIGN

A complete solar and terrestrial radiation measuring system ideally consists of the following seamlessly integrated components:

- *Instruments: SW / LW and peripherals*
- *Maintenance (inspection and calibration routines)*
- *Data management strategy*
- *Communication with (international) database.*

In an ideal system design, integration strategies between components are sought, driven by the strict implementation of a design plan. However, this was not the case with BSRN - as discussed in Section 2.1 and pointed out by Mc Arthur (1995). This unique process was driven by utilization and upgrading of existing installations in continuous feed-back and learning. This also explains the frequent referrals to real situations incurred in this Chapter.

3.1 INSTRUMENTS

In the design of a measurement system, knowledge of pre-measurement processes have to be incorporated. These processes are combined with identification and the best possible quantification of sources of known error to be applied in the final step. The remedies for the sources finally need to be characterized and quantified to the extent that their application will add value to the eventual measurements.

Knowledge of the different radiation components is necessary, as well as their possible sources of error. These sources of error can be either eliminated or meaningful corrections can be applied, in order to minimize the impact of those errors in the final quality of archived or presented data. It is a known fact, that all measurements inhibit a certain degree of uncertainty, in fact, without expressing the uncertainty of a measurement, it lacks worth and credibility (Cook, 1999).

The art of making measurements is therefore to strive towards entertaining the minimum amount of uncertainty.

Figure 3.1 features the basic components of a typical radiation site layout (as found at the De Aar BSRN site).

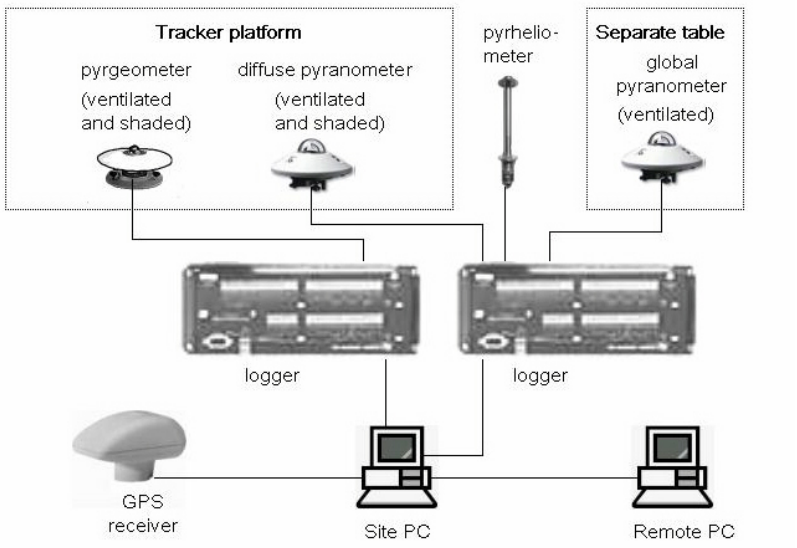

Figure 3.1 *Schematic layout of basic instrumentation at a BSRN site*

Each component, as well as the system as a whole, have its own unique sources and ways of inducing uncertainties in the eventual measurements. A system is indeed only as strong as its weakest link, so all of these factors, and in particular the sources of error, need to be taken into account when realizing a measurement programme and maintenance schedule.

3.1.1 Aspects of pyrheliometers

Pyrheliometers form the basis of SW measurements at a radiation site in general and a BSRN site in particular, as discussed in Section 2.5.2.

3.1.1.1 Operational errors

A pyrheliometer needs to be pointed towards the sun continuously, requiring a secure mounting on a solar tracker device, which, in turn, executes a reliable programme following the daily solar track in the sky. Any initial misalignment in either the tracker setup, mounting

of the pyrheliometer or any other form of error in the execution of the solar tracking may cause the pyrheliometer not to point exactly towards the sun, and subsequently yield erroneous readings.

This point is illustrated in Figure 3.2. A misalignment between the twin De Aar pyrheliometers (A and B) occurred during the morning of 26 January 2003 prior to about 10:00 UT. The sunspot of pyrheliometer A became misaligned by a discernible amount, similar to a routine tracker drift experienced, because the tracking system is passive. At the same time, and on the same tracker, pyrheliometer B remained in the correct position during this period. The outputs of pyrheliometers A and B are plotted against the left-hand Y-axis, in W.m^{-2}. The difference B minus A is plotted against the right-hand Y-axis, also in W.m^{-2}. Pyrheliometer B was restored to its correct position at about 10:00 UT.

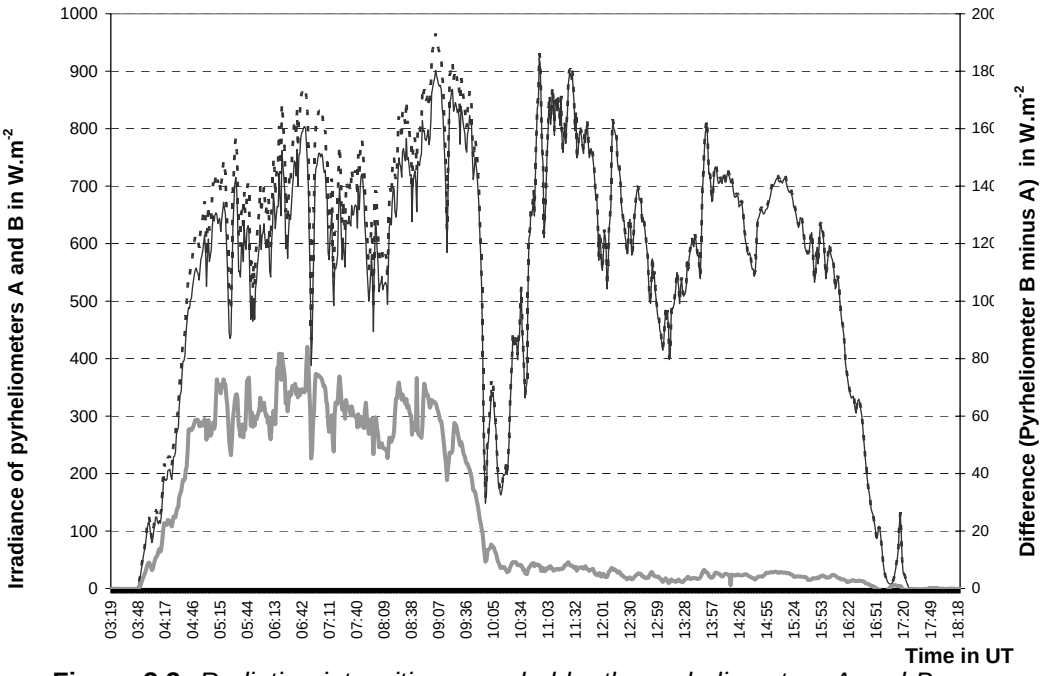

Figure 3.2 *Radiation intensities recorded by the pyrheliometers A and B, as well as their difference (B minus A) on 26 January 2003.*

During the period prior to the recovery, a difference of about 60 W.m^{-2} was observed, whilst after the recovery, it diminished to less than 10 W.m^{-2}. The 60 W.m^{-2} error exceeds the accuracy standards discussed in Section 2.2.2 by a substantial margin, emphasizing that correct tracking alignment is of paramount importance.

Tracker drifts are also addressed in Section 3.1.4 where the concept of double pyrheliometers is used in an attempt to address this issue. Double pyrheliometric measurement also aids in identifying cleaning times, as discussed in Section 3.1.5.

Another source of error is an unclean window, either from the outside (dirt collecting) or inside (moisture condensation). This can be rectified and should ideally be prevented by sound operational techniques and a regular inspection routine, leading to early identification and employing rapid remedial procedures.

Due to prolonged exposure to the solar radiation it is measuring, the instrument thermopile deteriorates with time. Typically, the black absorbent surface of the thermopile develops a shining surface leading to the thermopile becoming slightly more reflective, hence absorbs less radiation and subsequently seems to lose its sensitivity (Van der Molen and Koshiek, 1995). The true instrument sensitivity will therefore deviate from the number quoted in the original calibration certificate, hence regular comparison against a reliable standard instrument (calibration) is necessary in order to use the instrument output as a true irradiance measurement.

Observed changes in pyrheliometer sensitivity at the De Aar site during the first three years of operation are listed in Table 3.1. The term "CH1" and the cited serial numbers refer to the pyrheliometer in use. Values are quoted in $mV.kW^{-1}.m^{-2}$. Note that the 1997 and 1999 values are the same, since factory calibration constants were initially used after installation.

Table 3.1 *Observed pyrheliometer sensitivities since the De Aar BSRN installation*

Calibration Date	Instrument CH1 serial number 970156	Instrument CH1 serial number 970157
14 July 1997	12.95	13.74
28 July 1999	12.95	13.74
25 January 2000	12.75	13.58
28 July 2000	12.70	13.55
24 March 2001	12.77	13.55
26 September 2001	12.79	13.55
28 March 2002	12.65	13.57
27 January 2003	12.62	13.44
Total Calibration Drift	2.55 %	2.18 %
Calibration drift per year	0.460%	0.394%

If no calibrations were done after the initial De Aar installation, the total calibration drift would translate to an error of 20 $W.m^{-2}$ in a typical reading of 800 $W.m^{-2}$. This also exceeds the required accuracy described in Section 2.2.2 by a significant margin, therefore, sustained and regular calibration is the most important aspect in BSRN site operation.

The sources of error mentioned so far are operational in nature, and by using proper observational techniques can, should and must be kept to a minimum for most of the time.

There are, however, other intrinsic errors and sources of uncertainties in pyrheliometric measurements that in principle cannot be avoided entirely. The approach towards these uncertainties and errors is not attempted elimination, but rather a management strategy to keep uncertainty to a minimum. Each of the following sub-sections highlights one of these errors.

3.1.1.2 Window errors

A window is usually mounted in front of a pyrheliometer to enable all-weather operation. Ohmura *et al.* (1998) refers to an investigation by a BSRN task team using cavity radiometers and several kinds of protective filters. It was found that the best protective filter is already blocking 23 $W.m^{-2}$ of radiation located in the LW region. In the 6.3 µm band (known for the absorption by water vapour), as much as 7 $W.m^{-2}$ is blocked. This implies, that uncertainties in water vapour absorption alone account for more than the 2 $W.m^{-2}$ uncertainty goal cited in Section 2.2.2, which thus becomes unattainable.

However, practical implications in operational circumstances call for the presence of a window. For continuous operation of normal incidence pyrheliometers, a window has to be fitted. This window protects the delicate thermopile from accumulation of dust, which would render it ineffective with time. It also prevents water from collecting in the tube when it is pointed skyward during a rainstorm, and the detrimental effects that the presence of moisture would have on the delicate interior parts.

Automatically closing, rain-triggered and motor-driven sheltering devices, as proposed and built by Heimo *et al*. (1993), were not an option at De Aar, due to the fact that they would not be effective and not warrant the high costs involved. Rainstorms in the Karoo are mostly of convective nature, and with low surface moisture. They are often driven by rapid and strong convective development, resulting in a large amount of rain falling, even before an automatic device would be able to close and shelter the radiometers.

The Infrasil I-301 window in front of the CH1 in operation at De Aar, has a theoretical cut off wavelength of 0.14 µm to 5.2 µm (9 eV to 0.24 eV) - (Cannas *et al.*, 2001, 2002). This is

well outside the bulk of the solar spectrum or the “meteorological radiation” interval of 0.3 µm to 3 µm. Therefore the manufacturer’s window was retained for the De Aar instruments.

3.1.1.3 Circumsolar radiation

The Sun - Earth distance varies by 3.4 % between the point of aphelion (152.6 million km) and perihelion (147.5 million km). This constitutes a theoretical solar disk size of between 0.52° and 0.54°, as seen by an observer on Earth.

The solar disk as observed from the Earth’s surface, however, appears to be larger, since atmospheric particulates, such as aerosols and water vapour, have a strong scattering ability. An annular area around the solar disk (solar aureole), is created by the atmospheric turbidity, radiating a certain amount of circumsolar radiation of which the inconsistency at any given moment is responsible for errors in the direct and diffuse radiation (Oliviéri, 1992).

The Kipp & Zonen CH1 (Figure 2.6.) deployed at the De Aar site has a full field of view, which is roughly ten times the diameter of the solar disk (5° ± 0.2°) to allow for interception of the entire apparent solar disk. A deviation of 0.75° from this ideal number is still within the tolerance limits (Kipp & Zonen, 1997a). A tenfold diameter means, that the area is hundredfold, therefore a 3% variation in a disk occupying 1% of the field of view, is not expected to have any significant impact on the measurements.

Research of circumsolar radiation by Major (1994 and 1995) describes the cavity radiometer’s penumbra and sky functions, dimension differences, as well as the exchange of LW radiation. This is necessary for the characterization of small differences for exact calibrations, such as those conducted by the WRR.

The De Aar pyrheliometers are kept within the 0.75° limit, as recommended by the manufacturer, as far as possible. When calibrating, the cavity radiometer is attached to the solar tracker and aligned for the calibration period using the manual sunspot-sights.

Variations in the solar output (e.g., due to the 11-year sunspot cycle) are in the order of a few parts per thousand (Frölich, 1989 and Willson *et al.*, 2003) and are expected not to play any significant role.

3.1.1.4 Thermal offsets

Thermal offsets influence all types of thermopile radiometers, including pyrheliometers. However, unlike pyanometers, the manufacturers have not attempted ventilation to try and equate sensor and instrument body temperatures. The CH1 instruction manual (Kipp & Zonen, 1997a) quotes an offset of 3 $W.m^{-2}$ in response to a change of 5 $K.h^{-1}$ in environmental temperature. The experience at De Aar is, that the pyrheliometer zero offset (presenting itself visibly during night-hours) is definitely smaller for pyrheliometers than pyranometers. In Section 3.1.2.3, thermal offsets in pyranometers are discussed.

3.1.2 Aspects of pyranometers

Pyranometer thermopiles are also exposed to prolonged exposure to solar irradiance leading to a loss of sensitivity rendering a need for frequent calibration.

A number of different methods to perform pyranometer calibrations were discussed by Forgan (1995), of which the simple method detailed in Mc Arthur (1998), involving global/diffuse swopping, is used at De Aar. The observed calibration drift in the operational BSRN pyranometers in $mV.kW^{-1}.m^{-2}$, since their installation at De Aar, is listed in Table 3.2. Note that the 1997 and 1999 values are the same, since factory calibration constants were used since the first installation.

Table 3.2 *Observed pyranometer sensitivities since the De Aar BSRN installation*

Calibration date	Pyranometer CM21 serial number 970442	Pyranometer CM21 serial number 970443
31 October 1997	19.68	23.36
28 July 1999	19.68	23.36
25 January 2000	19.60	23.00
28 July 2000	19.55	22.84
24 March 2001	19.50	22.84
26 September 2001	19.41	22.70
28 March 2002	19.29	22.68
27 January 2003	19.27	22.49
Total Calibration Drift	2.08 %	3.72 %
Calibration drift per year	0.397%	0.710%

Since installation, the same two pyranometers were in operation, regularly swopped after every calibration episode. Between calibration periods they are used alternatively as global and diffuse instruments, following the recommendation by Forgan (1996). This way of calibrating and operation was in fact the only option for De Aar, since the initial instrumental consignment only included two CM21 pyranometers, and there were no other similar pyranometers in possession of the SAWS at that stage.

3.1.2.1 Operational errors

The impact of operational errors should be kept as small as possible for BSRN measurements. These errors include the following:

- The pyranometer has a built-in sprit level that is preset at the factory to be precisely aligned in all directions to the thermopile (radiometric levelling). A correctly set bubble level on site is assumed to render a perfectly level thermopile.

- The diffuse pyranometer needs to be mounted on the rotating solar tracker platform in order to make use of the solar shading device for diffuse measurements. However, the platform is subject to being slightly off-balance at a given moment due to a certain amount of play induced in the tracker. The impact of off-balance pyranometers is less pronounced in diffuse pyranometers, because of the smaller overall signal (Ohmura *et al.*,1998).

- The accumulation of dirt and other deposits on the outer dome over time leads to erroneous readings. As with pyrheliometers, this is effectively neutralized by regular inspection (at least once per day) and subsequent dome cleaning, also after rainstorms, by site staff.

- If water enter the pyranometer either by moisture condensation or precipitation, the interior metal parts can corrode. This problem is addressed by the presence of dessicant granules in a small cavity in the body, extracting moisture. Granules are self-indicating, being typically pink in the presence of a certain amount of moisture and blue if dry.

- Shading errors, as a result of tracker errors or independently thereof, as a result of changing shading device geometry, lead to incorrect exposure of the diffuse pyranometer and erroneous readings. The disk should correspond to the field of view of the pyrheliometer to allow for correct application of the relationship global/diffuse/direct, but on the other hand, should also be adequately oversized (Heimo, 1993), so that small drifts encountered during unattended operation do not lead to large errors. Infrequent inspection due to rainy weather lasting for several days, can lead to a large shading error not being timeously identified. At De Aar it is highly unlikely since bad weather does not occur in long successions, and frequent inspection visits by site personnel are possible.

3.1.2.2 Cosine error

Ideally, a horizontally mounted pyranometer would measure radiation I, incident at a zenith angle Z, as a fraction of $I.cosZ$, for all angles between 0° and 90.83° (when the sun rises or sets). All radiometers, however, deviate from this ideal and its quantity is defined as the cosine error (Schreder *et al.*, 1998), expressed in Equation 3.1:

$$f_1(Z,\theta) = 100\{\frac{F(Z,\theta)}{F(Z=0°,\theta).\cos Z} - 1\} \qquad (3.1)$$

where Z = Incident (zenith) angle, measured between the level of incidence and a line normal to the horizontal level

θ = Azimuth angle

F = Radiometer's reading in nominal units at angles Z and θ, respectively

According to the manufacturer, CM21 pyranometers deployed at the De Aar site have a maximum cosine error of 1.3% at solar elevation of 10°. This translates to an error of less than 13 W.m^{-2} for global radiation at 1000 W.m^{-2} or an error of less than 4 W.m^{-2} for diffuse radiation of 300 W.m^{-2}. This compares positively with earlier Kipp & Zonen pyranometers, for which an error of -4% to +8% in the CM3 and 0.4% to 2.0% in the CM11 was the norm (Kipp & Zonen, 1992, 1995).

At low solar angles, the accuracy of global radiation is degraded by cosine errors (Augustine *et al.*, 2000). This is one of the motivations in the BSRN context for defining global radiation

(DSGL1) as the sum of diffuse (DSDFS) and normal direct (DSDIR * cos Z, where Z = solar zenith angle) radiation, as discussed in Section 2.5.4.

3.1.2.3 Thermal offsets

One weakness of pyranometers, is its susceptibility towards environmental temperature fluctuations and an induced phenomenon known as thermal offsets. This was the topic of thorough investigation and extensive documentation by authors, such as Smith (1999) and Dominguez (2001), who devoted entire dissertations to this topic. This offset quantity draws attention in the measured night-time quantities as a negative pyranometer signal in the absence of a solar signal. Hence the alternative term “night-time offset” or “zero offset”.

When the pyranometer dome is exposed to a “cool sky” (clear), mostly, but not necessarily at night, the pyranometer dome cools rapidly. This happens, because the radiometer dome has a large area exposed to the sky and only a small thermal mass with which to resist cooling. The cooling is transferred to the inner dome and thermopile, while the instrument body, unlike the dome, has large thermal inertia and does not cool off as quickly. This results in a reversed signal between the relatively warm body and the relatively cool thermopile, which is interpreted by the data acquisition system as a negative radiation quantity.

The negative quantity is not restricted to night-time measurements, as shown by the above authors. The impact of this error therefore has implications for present, as well as past pyranometer-generated daytime records, since a worldwide under-estimation of global, as well as diffuse quantities in climate records exists (Philipona, 2002). This was only discovered by combining measured and calculated quantities, using radiative transfer models. A responsible approach to the counteraction of thermal offsets should therefore be followed.

One such approach is proposed by Haeffelin *et al*. (2001). When thermistors are placed in the “cooling path”, thermal characteristics of the cooling components can be determined and accurate models to calculate the expected offset can be developed empirically. However, this approach requires, that the radiometers are dismantled and re-assembled again, which was not an option for SAWS.

A more common practice, also adopted at De Aar, is artificial ventilation (in terms of dedicated ventilators by the manufacturers) in a constant air stream over the instrument dome. This is an attempt to keep the dome temperature in synchronization with the ambient temperature, and ventilators ideally provide sufficient airflow to counteract the thermal offset.

However, there were times when the ventilators did not function. One such incident of notable proportion was the interruption in ventilation between 10 and 26 January 2003, as a result of lightning damage to the power supply unit on 8 December 2002.

The unventilated pyranometer output for this period is plotted against the global pyranometer (Figure 3.3) and the diffuse pyranometer (Figure 3.4) in two separate scatter-diagrams, as suggested by Dutton *et al.*, (2001).

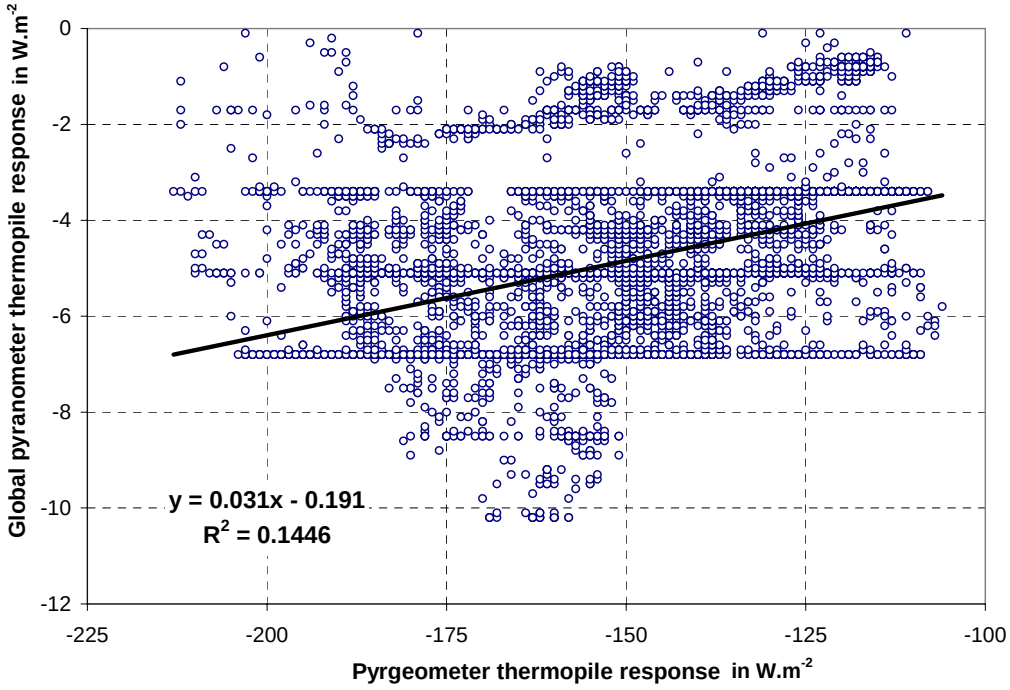

Figure 3.3 *Scatter plot for global pyranometer thermopile response versus pyrgeometer thermopile response for 10 to 26 January 2003*

Regression lines were drawn in both cases, but the R^2 correlation values are low and only a faint linear relationship between thermopile reactions of the pyrgeometer versus either the global or diffuse pyranometers exixts. The relatively large thermal offset errors during this period are well outside the pyranometer uncertainty goal, as discussed in Section 2.2.2.

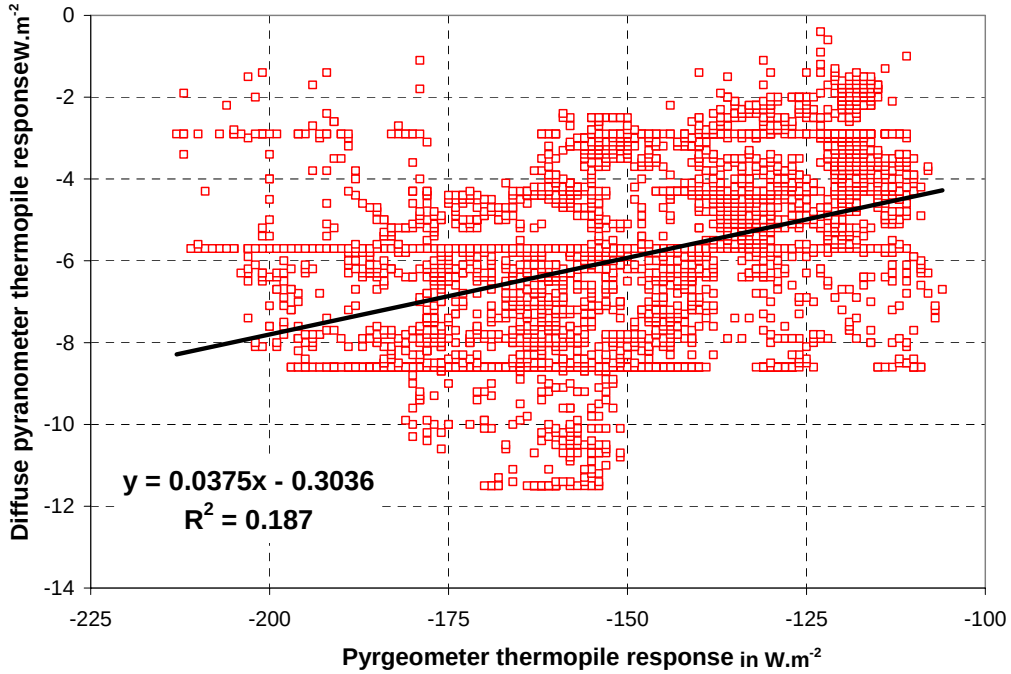

Figure 3.4 *Scatter plot for diffuse pyranometer thermopile response versus pyrgeometer thermopile response for 10 to 26 January 2003*

Another method to counteract thermal offsets is implemented by the Australian Bureau Of Meteorology (BOM). No artificial ventilation is applied and compensation for the measured quantities is calculated retrospectively, as described by Forgan (2001). This method has the following advantages:

- The system does not depend upon the proper functioning of ventilators, which have an uncertain reliability and efficiency.
- The compensation method, as detailed by Dutton *et al*. (2001), may be applied using only the thermopile outputs of the pyranometer and the pyrgeometer.
- This method also compensates for day-time thermal offset errors, which are difficult to determine otherwise.
- With no ventilators running, less power is consumed by the system.

3.1.2.4 Artificial ventilation and/or heating.

If snow or ice forms on the pyranometer dome, the option exists to heat the ventilating air with 5 W or 10 W, but not raising the ventilated air temperature by more than 0.1°C per W (Kipp & Zonen, 1994). However, for De Aar, having only 0.8 snow days per year (SAWB, 1986), the introduction of artificial heat is not justified. Winter is associated with dry air in an anticyclonic circulation over the interior of the country, including the De Aar region. The surface dewpoint is therefore in general so low that frost hardly forms.

Artificial ventilation has the advantage that the formation of dew and frost on the sensor dome is reduced, since there is a constant airflow and subsequent evaporation of any moisture droplets forming on the dome. However, care should be taken, that ventilation is not too strong, since significant measurement errors can be induced if the air flow is more than 3 $m.s^{-1}$ (Koshiek, 1996). Cleaning should also be done often because the added ventilation causes forced evaporation of moisture. If this moisture attracts atmospheric dust, it leads to a build-up of a thin layer of dirt (Kuik, 1997).

3.1.3 Aspects of pyrgeometers

The instrument used at De Aar for measuring surface LW radiation fluxes (wavelength more than 3.5 µm) at De Aar is the PIR, as discussed in Section 2.5.5 and featured in Figure 2.7.

The thermopile output of an upfacing PIR pyrgeometer was in first principal assumed to be proportional to Longwave Downwelling radiation (LWD), in a ratio equal to the thermopile's sensitivity to LW radiation. This approach led to erroneous measurements as described by authors such as Enz *et al.* (1975). The main cause of error was excessive solar heating of the (dark) instrument dome, re-radiating a significant amount of LW radiation from the dome towards the thermopile, resulting in measurements larger than true atmospheric LWD.

In an attempt to counteract radiative effects of the dome, a "compensation" circuit, as described by Fairall *et al.* (1998), was introduced to Eppley pyrgeometers. This circuit was meant to have an output equal to the dome radiative effect, so that when the circuit's output is superimposed upon the thermopile output, only true LWD is measured. Unfortunately this circuit is powered by a separate conventional dry cell battery, which is drained by the circuit relatively fast, leaving uncertainty as to the true amount of "compensation" it provides.

The big disadvantage is that no rectification of "data under suspicion" can be done afterwards, since the thermopile output is not recorded separately from the compensation circuit.

The BSRN community hence rejected the usage of the compensation circuit (WCRP-54,1991) and recommended that the effects are compensated for in an equation (3.3). The thermopile of a shaded ventilated pyrgeometer plus accurate individual temperatures of the metal body (case) and silicon-coated dome are used for this calculation. This Equation was introduced by Philipona *et al.* (1995):

$$E_{LW} = \frac{p}{C_1}(1 + k_1\sigma T_b^{\,3}) + k_2\sigma T_b^{\,4} + k_3\sigma(T_b^{\,4} - T_d^{\,4}) \qquad (3.3)$$

where

- p = thermopile millivoltage directly measured (expected to be -0.8 mV to 0.1 mV)
- C_1 = thermopile long-wave sensitivity constant (around 4 mV.W.m^{-2})
- σ = Stefan - Bolzmann constant
- T_b = instrument body (case) temperature
- T_d = instrument dome temperature
- k_1, k_2, k_3, = empirical constants

The exact values for k_1, k_2 and k_3 are unique for every instrument and can only be determined during an absolute controlled calibration (characterization) of a pyrgeometer - something that few BSRN sites have access to, or can even afford. However, if one assumes k_1 = 0, k_2 = 1 and k_3 = 3.5 , Equation 3.3 simplifies to

$$E_{LW} = \frac{p}{C_1} + \sigma T_b^{\,4} + 3.5\sigma(T_b^{\,4} - T_d^{\,4}) \qquad (3.4)$$

Equation 3.4. is in fact an earlier pyrgeometer equation described by Albrecht and Cox (1977), which was in common use for 18 years before Equation 3.3. was derived. Since SAWS do not have access to an absolute pyrgeometer calibration, Equation 3.4. was the more likely choice for LWD at De Aar. It was however, decided to perform an error analysis between Equations 3.3 and 3.4, using typical De Aar values for the variables, to quantify the expected error using Equation 3.4. instead of Equation 3.3.

3.1.3.1 Error analysis between two equations

Both equations consist of three terms, each characterized as follows:-

- Term 1: ($\frac{p}{C_1}(1+k_1\sigma T_b^{\,3})$ in Equation 3.3 or $\frac{p}{C_1}$ in Equation 3.4) equals net LW irradiance (upwelling LW minus downwelling LW).

- Term 2: ($k_2\sigma T_b^{\,4}$ in Equation 3.3 or $\sigma T_b^{\,4}$ in Equation 3.4) is the physical pyrgeometer body heat Term. This is just the application of the Stefan-Bolzmann equation to the pyrgeometer exposed to the sky as a blackbody radiator.

- Term 3: ($k_3\sigma(T_b^{\,4} - T_d^{\,4})$ in Equation 3.3 or $3.5\sigma(T_b^{\,4} - T_d^{\,4})$ in Equation 3.4) is the dome compensation Term. When the instrument is in operation, this Term is relatively small as a result of continuous shading of the instrument dome, leading to a small difference between T_b and T_d. Therefore, uncertainties in Term 3 as a result of 3.5 not being the exact number, are kept to a minimum.

Each of the terms is individually and exclusively influenced by the k-values: The error in k_1 will only influence Term 1, likewise k_2 only Term 2 and k_3 only Term 3. This means that the overall error can be assumed to be the sum of the errors for the respective terms.

The following long-term means applicable to Equation 3.4, were measured at De Aar:

- p = 0.713 mV
- C_1 = 0.000427 mV.W^{-1}.m^2
- T_b = 297.9 K
- T_d = 296.3 K
- E_{LW} = 312.9 W.m^{-2}

These numbers were used to evaluate the three terms of Equation 3.4 as -167.0 W.m^{-2}, 446.6 W.m^{-2} and 33.3 W.m^{-2} respectively. Note that the sum of these terms equals the long-term average of 312.9 W.m^{-2}.

The same long-term average values, as quoted above, were used to evaluate Equation 3.3, together with typical values for k_1, k_2 and k_3 found in absolute characterizations for the same PIR instruments used by Hirose (1998) and Philipona (1995). The errors in E_{LW}, using Equation 3.4 instead of Equation 3.3, was calculated for both the minimum and maximum of the Hirose and Philipona numbers, to set borders in the errors and show the range of these errors. These maximum and minimum errors were calculated term by term as the absolute (percentage) errors. In a further step, they were multiplied by the relative term size in the total LWD, to be normalized as relative (weighted) term errors, shown in Table 3.3.

Table 3.3. *Error estimation using Equation 3.4 for typical De Aar values instead of Equation 3.3*

Term	Equation 3.4		Equation 3.3				Absolute term error		Relative term error	
	Value for k	Term size in W.m^{-2}	Value for k		Term size in W.m^{-2}					
			Min	Max	Min	Max	Min	Max	Min	Max
Term1	0	-167.0	0.053	0.138	-180.2	-191.3	-7.94 %	-14.5 %	-4.72 %	-8.63 %
Term2	1	446.6	1.0024	1.0198	447.6	447.6	0.24 %	1.98 %	0.35 %	2.86 %
Term3	3.5	33.3	2.5	4.3	23.8	40.9	-28.6 %	22.9 %	-2.95 %	2.36 %

The sum of the extreme relative errors, irrespective of whether such an extreme is the result of the maximum or minimum value for k, now yields a "worst case scenario" percentage for both extremes, -11.24 % and 0.50 % respectively. The overall mean error using Equation 3.4 instead of Equation 3.3. is therefore the mean between these extremes. i.e. -5.37 %. This translates to 16.8 W.m^{-2}, using the long-term LWD average. It should be noted that it exceeds the range discussed in Section 2.2.2.

From Table 3.3 it became obvious that the main contributor to this error is Term 1, or more specifically, the fact that k_1 = 0 is used instead of a more realistic number between the typical values of k_1 = 0.053 and k_1 = 0.138.

3.1.3.2 Relative contribution of terms in LW equation

The significance of each of the three terms in Equation 3.4 is now illustrated by choosing representative days in different seasons and sky conditions. Continuous midnight-to-midnight plots of one-minute values of Term 1, Term 2 and Term 3, as well as LWD (sum of terms) are presented in Figures 3.5, 3.6, 3.7 and 3.8. All times are quoted in Universal Time

(UT). Note that South African Standard Time (SAST) = UT + 2 hours throughout the year. Figure 3.5 depicts a clear sky winter day (2 June 2000).

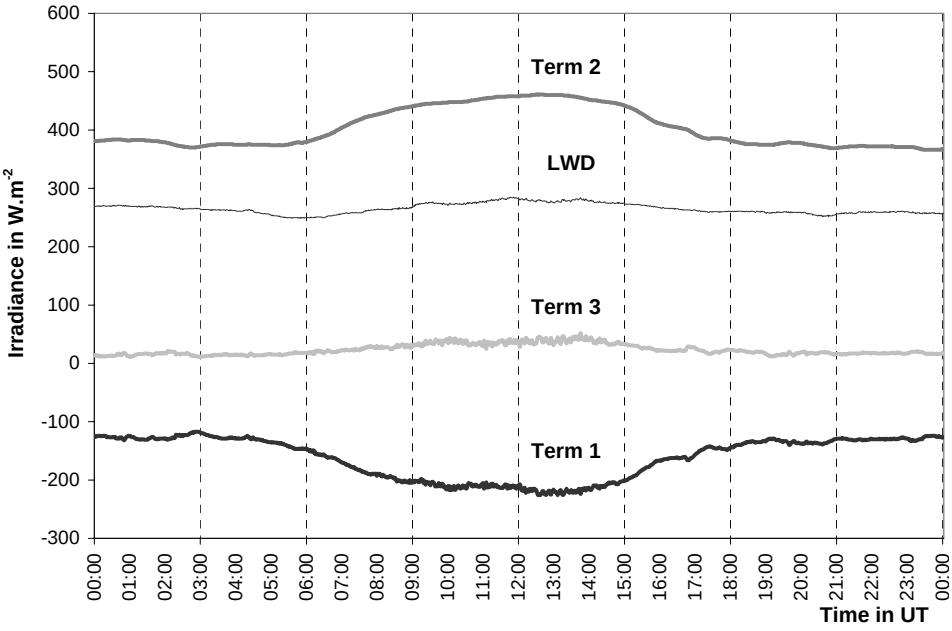

Figure 3.5 *Individual LWD term contribution on 2 June 2000*

The weather experienced on this day is typical for the country's interior during the winter. The diurnal pattern of atmospheric heating, starting at sunrise (05:14 UT) and ending at sunset (15:30 UT) is reflected in Term 2, while Term 1 is almost an exact mirror-image of Term 1, i.e., a classic example of "what goes in also goes out". The steadiness of Term 3 in proportion to the other terms, also results in the flat line for LWD. For this day, the minimum LWD = 249 $W.m^{-2}$, while the maximum LWD = 285 $W.m^{-2}$, hence the range of LWD for that day (maximum minus minimum) is only 36 $W.m^{-2}$.

Figure 3.6 (A partly cloudy winter day, 22 June 2000), shows the profound effect that clouds have on the measurement of LWD. Compared to 2 June 2000, sunrise is now 7 minutes later (05:21 UT), and sunset virtually at the same time (15:31 UT). Term 2 shows the same diurnal pattern than in Figure 3.5, but with a downward slope towards the late afternoon, which can be attributed to the presence of clouds.

For all three terms, as well as LWD, the values are similar to those of Figure 3.5. An exception is Term 3, which shows more features embedded in a relatively straight line. By far the biggest contributor to the differences between Figures 3.6 and 3.5 is Term 1. Notice how the characteristics of Term 1 are almost mirrored in LWD for that specific day. The presence of clouds prevents the emmission of LW radiation and leads to an overall higher

LWD level, although gaps in the clouds allow for emmissions, such as the “dip” between 12:50 UT and 13:50 UT.

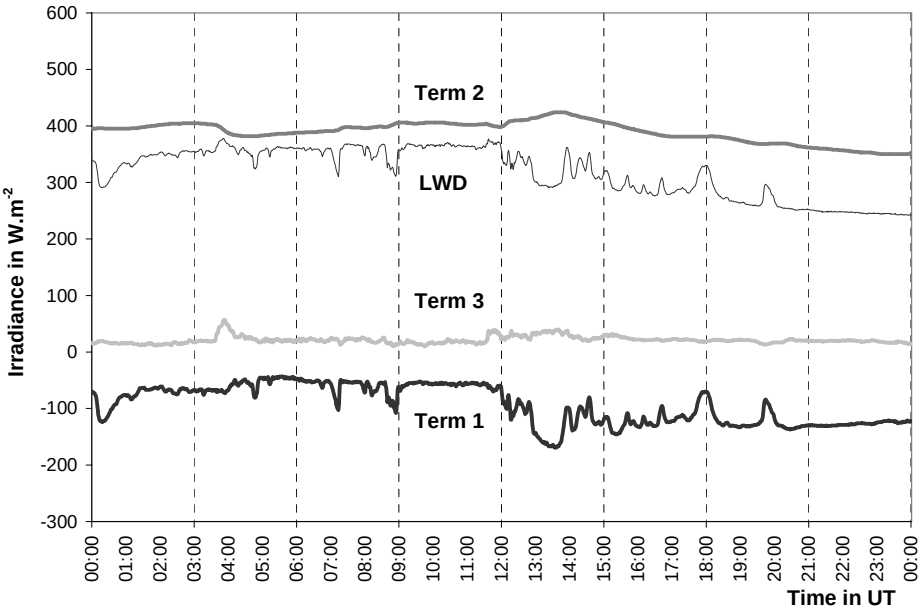

Figure 3.6 *Individual LWD term contribution on 22 June 2000*

Perfect clear-sky days in summer are rare and Figure 3.7 (30 December 2000) depicts a summer day with only thin clouds present - for all intents and purposes, a clear sky day.

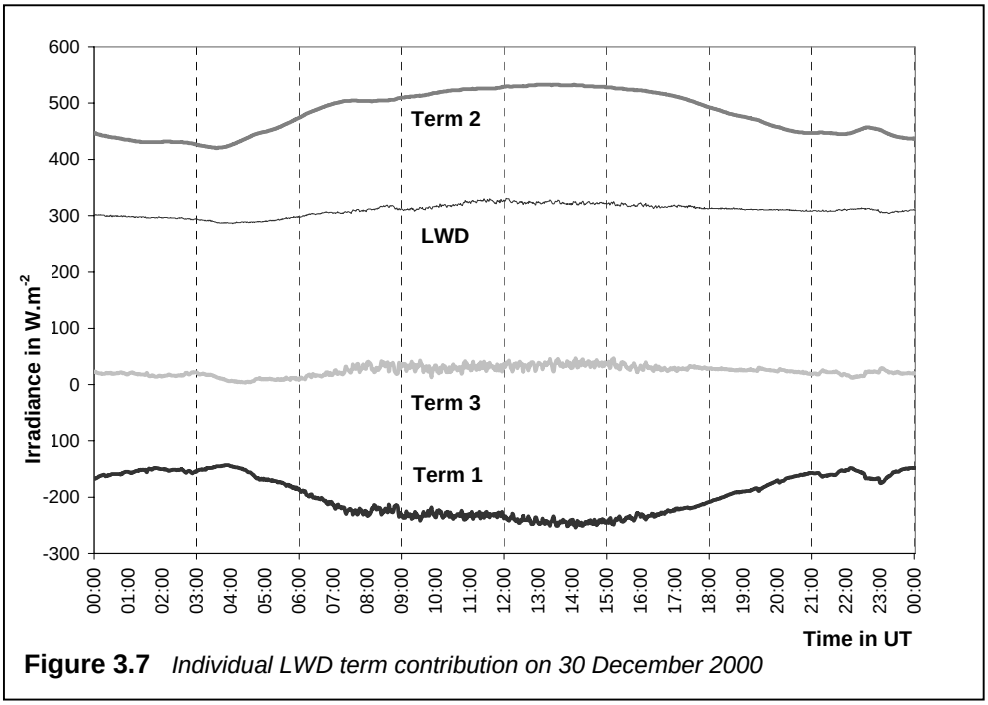

Figure 3.7 *Individual LWD term contribution on 30 December 2000*

The same pattern as in Figure 3.5 is present here, although sunrise occurs already at 03:23 UT and the sun sets at 17:30 UT. A longer day and more perpendicular incident SW

radiation is reflected in overall higher values for Term 2. This is mirrored in the same way as in Figure 3.5 through lower values in Term 1, since the incident SW radiation is re-radiated again almost in its entirety as LW radiation. Minimum LWD = 292 W.m^{-2}, Maximum LWD = 375 W.m^{-2}. The range of LWD is 83 W.m^{-2} for this clear summer day, compared to 36 W.m^{-2} for the clear winter day.

Figure 3.8 (11 December 2000) is the classic example of a summer day where clouds developed during the course of the day and either precipitated at the site, or drifted away, clearing towards the late afternoon.

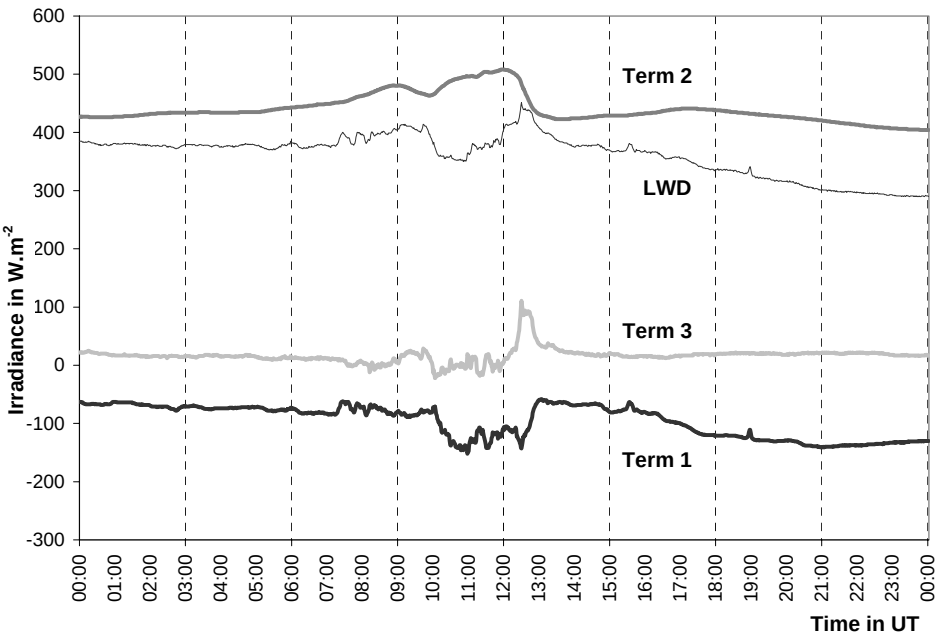

Figure 3.8 *Individual LWD term contribution on 11 December 2000*

From sunrise at 03:14 UT up to 08:00 UT, the SW radiation input increases and Term 2 shows a smooth and steady rise. Between 08:00 UT and 10:00 UT, cloudiness introduces features to Term 1 similar to those of a cloudy winter day (Figure 3.5), while Term 2 shows a marked decrease between 08:00 and 09:00. Between 10:00 UT and 13:00 UT, cloud cover increases and there was mild precipitation between 13:00 and 13:20. The prominent peak in Term 3 during this time, can be attributed to thermal shock as a result of the precipitation (cool water on the hot dome).

With the sky now clear after the mid-afternoon storm, Term 1 steadily decreases after 13:20 UT along with a more or less similar smooth line that can be seen prior to 08:00 UT, as the earth cools down and radiates long-wave radiation. Term 2 does not respond likewise, since the sun is already low at this stage and about to set. After sunset, (17:20 UT) a change in

the steady slope of Term 1's decline can be seen, leading to LWD values lower than during the corresponding summer clear sky day in Figure 3.7.

3.1.3.3 Artificial ventilation and/or shading

Modern operation of the pyrgeometer requires continuous shading of the dome, since SW radiation is easily absorbed by the dark dome, leading to heating, false secondary radiation towards the thermopile (Ji *et al*., 2000), and subsequent false signals.

The reason for ventilation of the pyrgeometer is the same as for a pyranometer, viz., equating the dome and "naked" thermopile temperatures as much as possible. In the case of the pyrgeometer, the ventilation also attempts to prevent a temperature gradient developing on the dome leading to false signals (Richardson, 2000). Philiopona (1995) showed, that pyrgeometer errors may largely be reduced by applying the Swiss modification, as discussed in Section 2.5.5.

Standard pyrgeometer and pyranometer ventilating devices were continuously operational at De Aar. The one exception is during power failures, which also resulted in tracker stoppages (Section 3.1.4.2). For the operational history of the De Aar BSRN station, tracker stoppages and ventilator failures are closely related.

3.1.4 Aspects of the solar tracking system

The presence of a shading ring to enable diffuse pyranometric measurements in the absence of solar tracking, was discussed in Section 2.5.3. However, the resultant data will have uncertainties due to the empirical and often inadequate correction factors that such a ring requires (Battles, 1995).

A ring and correction factors are not necessary for De Aar since the Sci-Tek two-axis solar tracking system comprises a shading device providing sufficient and continuous shading for the diffusometer (diffuse pyranometer) and pyrgeometer. However, the accuracy of all measurements except global radiation, therefore relies heavily on the accuracy of the tracker, and special care should be taken that the tracking device is accurate at all times.

Tracking failures have occurred for the following reasons since inception of the De Aar site:-

- Stopping of the solar tracking system due to power failures as a result of a combination of lightning strikes and/or routine maintenance on the municipal electricity supply leading to exhaustion of the Uninterrupted Power Supply (UPS).

- Power switched off during preparations for calibration and other site maintenance.

- Temporary misalignment of either the pyrheliometer or shading device.

3.1.4.1 Tracker misalignments

An active solar tracking system constantly observes the sun through a special series of sensors, which are aligned perfectly with the instruments. The sensor outputs constantly adjust the tracker drive motors and alignment in a feedback process for perfect solar tracking. A passive solar tracking system makes use of calculations of the solar position, and subsequent movement of the tracker motors to follow the sun "blindly".

An ideal solar tracking system is a passive system by default, able to switch to "active" mode when the sun is visible, and able to switch to passive mode when there is no visible sun.

The De Aar tracker is entirely passive, therefore regular inspections (three times a day, i.e., once near solar noon, once in the morning and once in the afternoon during about 45° solar elevation), are necessary to identify and rectify solar tracking errors.

One way of proactively addressing the effects of tracker errors, is to use redundant pyrheliometers. In Section 3.1.1.1 and Figure 3.2, the effect of a misalignment was illustrated and discussed. Taking readings from *both* pyrheliometers instead of one and picking the higher reading per recording interval, calls for a better aligned instrument every time. The philosophy of rather taking the best measurement of a given signal than the best measurement per individual instrument, (even if that signal arises from two different instruments; Ohmura *et al.,* 1998), is applied here.

In Figure 3.9, the readings for two (slightly) misaligned pyrheliometers are featured. By taking the higher of the readings, a better reading for direct radiation is obtained.

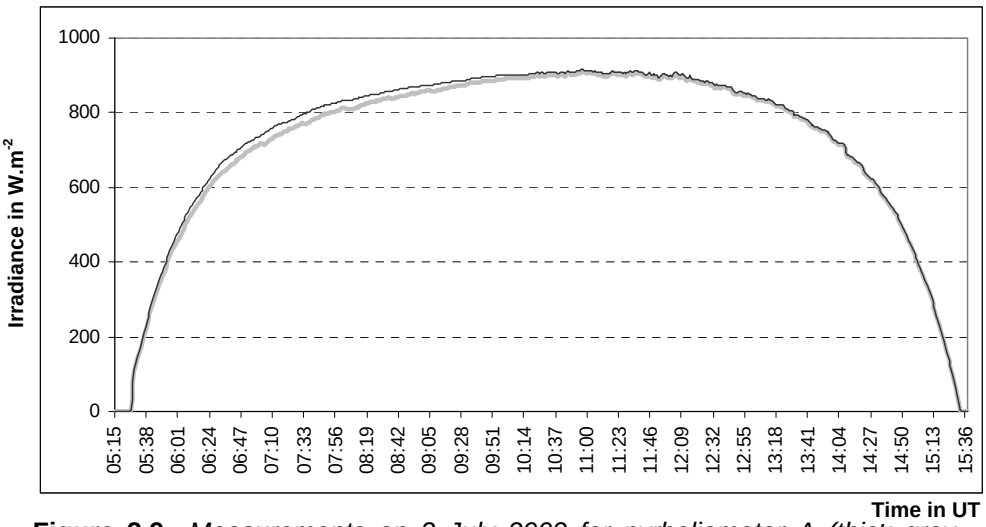

Figure 3.9 *Measurements on 2 July 2002 for pyrheliometer A (thick grey line), misaligned with pyrheliometer B (thin black line).*

3.1.4.2 Tracker stoppages

The best and only way to identify such occurrences is prompt and accurate reporting, backed up by skilled attendance to the problem. Using recorded data alone in an attempt to identify erroneous data is not the best way to correctly identify such events. An example of dealing with data from a prolonged tracker failure resulting from a power failure is shown in Figures 3.10 to 3.13.

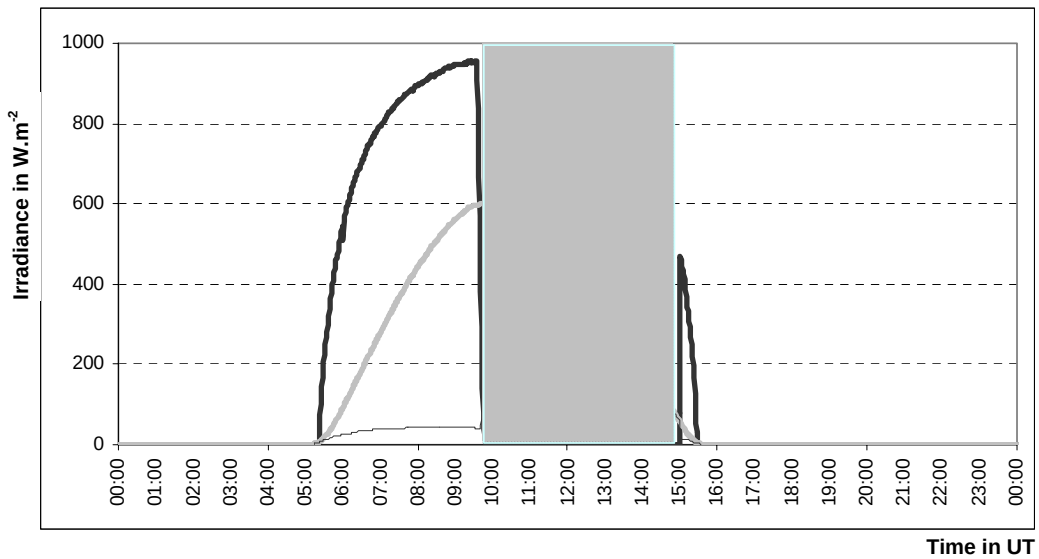

Figure 3.10 *Time-series for direct (thick black line), global (thick grey line) and diffuse (thin black line) radiation for 9 June 2002. The period of tracker failure is shaded.*

On 9 June 2002, maintenance on the commercial power lines commenced at 06:00 UT and the UPS was exhausted by about 10:00 UT. The power was restored at 15:00 UT.

In Figure 3.10, the impact of tracker failure is best illustrated in plots of SW radiation. The day was almost entirely cloud-free, except for a small incident of what appears to be scattered clouds, between 13:20 UT and 13:50 UT. This, however, did not interfere with what is intended to be illustrated here. The shaded area represents the period when the tracker stood still. Note that, immediately after the UPS power failed, output from the diffuse sensor increased sharply to co-incide with the global, while the direct radiation dropped to zero.

Now consider the equation

$$global(t) = diffuse(t) + direct(t)\cos Z \qquad (3.5)$$

where Z = solar zenith angle

in the context of

- DSGL2 = global radiation measured by the unshaded pyranometer
- DSGL1 = global radiation calculated using diffuse and direct radiation

Equation 3.5 then translates to

$$DSGL2 = DSGL1 \qquad (3.6)$$

Equation 3.6 should be valid before, after and during the tracker failure, as pointed out by Mc Arthur (1998), except for a small glitch on the moments of transition, due to different instrument reaction times. The "glitches" can be used to highlight the times of tracker failure. Consider a time-series graph of DSGL2 / DSGL1 for the same day shown in Figure 3.10.

For the entire day, including the period of tracker failure, DSGL2 / DSGL1 is close to 1 (Fig 3.11), with only a slight offset prior to tracker failure. The sharp "spikes" appear at sunrise (05:17 UT), sunset (15:29 UT) and to a comparable extent at the edges of the tracker failure times, indicated by the shaded area in Figure 3.11.

Since diffuse and direct instruments incur a "shock" signal during events such as tracker failures (diffuse exposed to higher than normal irradiance and the direct to less than normal), the different response times to adjust to normal leads to spikes similar to the sunrise/sunset spikes along the shaded areas represented in Figure 3.11. If "shocks" are used to identify tracker failure times, it would have limited use, since the "shock" effect would be masked in

partly cloudy to cloudy conditions where natural "shocks" of the same magnitude, can overrule the "shock" effect results from tracker failure.

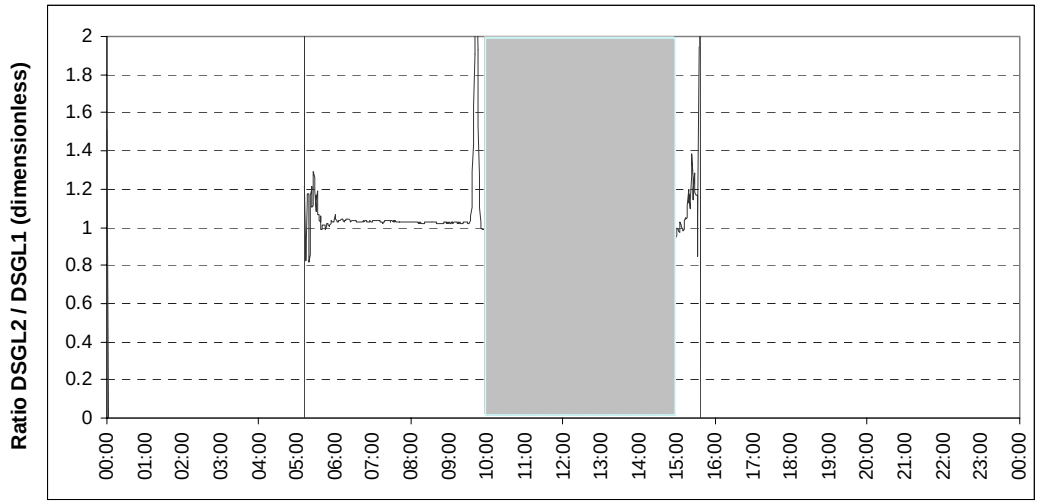

Figure 3.11 *Time-series of the ratio DSGL2/ DSGL1 for 9 June 2002. Tracker failure time is shaded.*

The tracker failure not only impacted on SW measurements, but also on the LW. The absence of shade on the pyrgeometer dome, leads to absorption of SW radiation, abnormally high temperature and re-radiation towards the thermopile, which receives a biased signal. In Figure 3.12, the values of the three terms of Equation 3.4, as well as LWD, are plotted for 9 June 2002. The shaded area represents the period of tracker failure.

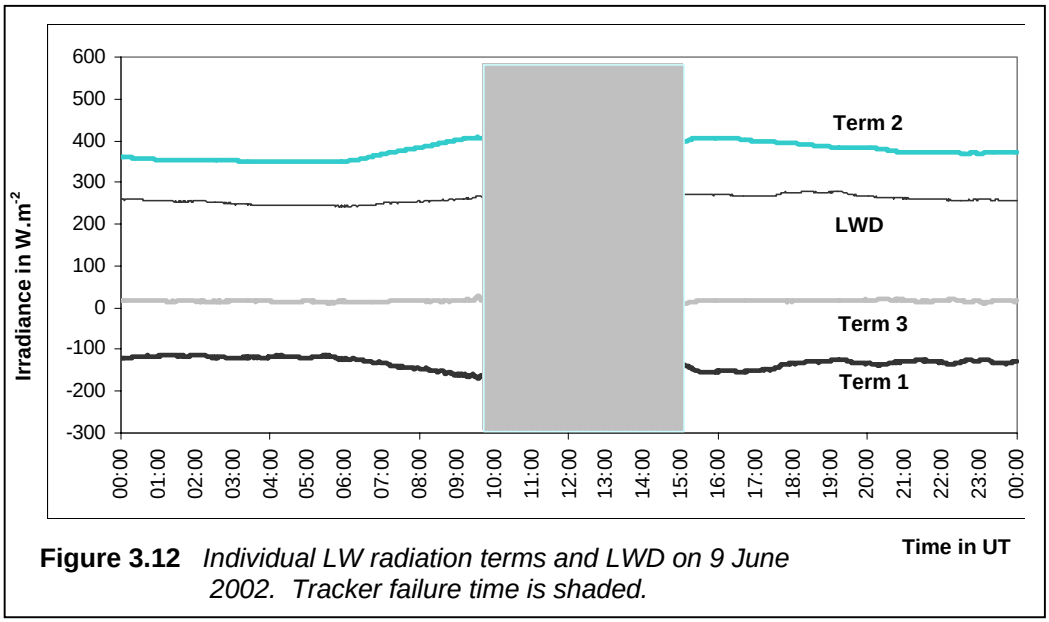

Figure 3.12 *Individual LW radiation terms and LWD on 9 June 2002. Tracker failure time is shaded.*

In Figure 3.12, Term 1 (the thermopile) shows a strong positive influence as a result of the solar heating. Term 2 (usually a smooth curve on a clear day, compared to Figure 3.5.)

shows signs of an impact from something else than LWD. Term 3 shows signs of an initial shock, recovering slowly. After shading is restored, it takes about half an hour to return to normal. Surprisingly little impact is shown on LWD using the scale of Figure 3.12.

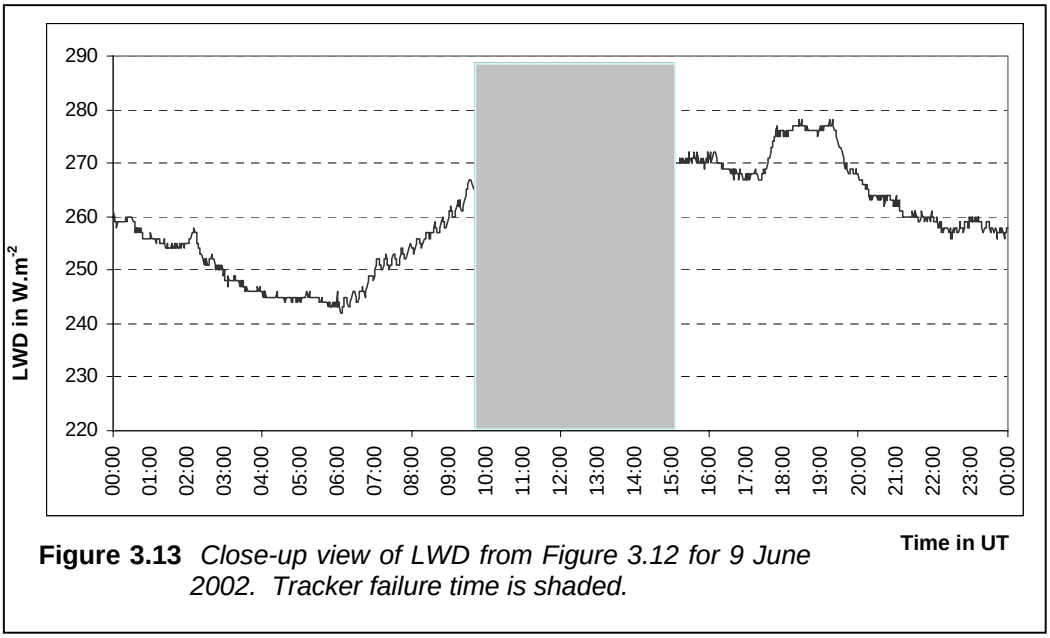

Figure 3.13 *Close-up view of LWD from Figure 3.12 for 9 June 2002. Tracker failure time is shaded.*

Figure 3.13 shows a closer view of LWD alone with an enhanced scale. A distinctive drop of about 10 $W.m^{-2}$ in LWD immediately after the tracker failure and a spike of about the same amount shortly before recovery, is observed.

3.1.5 Identifying instrument cleaning times

Normal station routine requires, that the time of daily dome and window cleaning is documented and reported. However, reporting instrument camp visit times and the subsequent deletion of data contaminated by human presence in the camp while cleaning the instruments often encompasses periods in the order of several minutes, for example ten. Normally one or two at the most of those ten minutes are truly unusable data. Here is a way of using the recorded data, to more accurately identify instrument cleaning times and serve to preserve more data.

As a result of the high 1 Hz sampling rate, the passage of a cleaning cloth over any of the sensors (even for a period of only one second) will guarantee that at least one sample less than the “true” irradiance is recorded. This false sample will reflect in the one-minute

statistics to different extents, depending on the sensor and the atmospheric conditions. Pyrheliometers reflect this effect maximally, given the narrow field of view. Thus, the cloth is expected to completely cover the aperture at a given moment and in principle a zero sample amidst a high irradiance level, is possible.

Redundant measurements for maintaining the record in case of occasional instrument failures for the many reasons instruments fail, are recommended (Mc Arthur, 1998). In the case of pyrheliometers, it can also be a means of identifying instrument cleaning times. The assumption is made that the human hand cleaning the two pyrheliometer windows, cannot do it simultaneously, and also is unlikely to spend exact time (up to the nearest millisecond) on each. Therefore those anomalies should be reflected in the data, and in particular, the standard deviation of the 1 Hz samples.

Table 3.4 lists a few succeeding one-minute averages (AVG) and corresponding one-minute standard deviations (OSD) for the two De Aar pyrheliometers, as well as for the diffuse and global pyranometers. The data was recorded between minutes 354 (05:54 UT) and 369 (06:09 UT) of day 186 of 2002 (4 July 2002). The OSD for the pyrheliometers, as well as the difference between the OSD for the two pyrheliometers, are shaded columns. The actual instrument cleaning time, is highlighted as a black row.

Table 3.4 *One-minute De Aar data for 4 July 2002 between minutes 354 and 369*

Year	Day of year	Minute of day	Pyrheliometer A		Pyrheliometer B		Diffuse pyranometer		Global pyranometer		Difference (N – M)
			AVG	OSD(M)	AVG	OSD(N)	AVG	OSD	AVG	OSD	
2002	186	354	276	0.5	284	0.5	24	0.0	50	0.8	0.0
2002	186	355	285	6.4	293	6.7	25	0.5	53	1.2	0.3
2002	186	356	300	2.0	308	2.0	26	0.6	56	0.3	0.0
2002	186	357	306	2.3	315	2.3	27	0.1	59	0.8	0.0
2002	186	358	314	2.4	323	2.5	27	0.0	61	1.5	0.1
2002	186	359	322	1.8	332	2.4	27	0.0	64	1.0	0.6
2002	186	360	327	1.4	340	2.1	29	1.0	66	0.2	0.7
2002	**186**	**361**	**330**	**17.6**	**345**	**11.2**	**30**	**0.3**	**69**	**0.6**	**-6.4**
2002	186	362	342	2.0	356	2.1	30	0.0	72	1.4	0.1
2002	186	363	348	1.9	362	1.9	30	0.0	74	1.0	0.0
2002	186	364	355	1.8	369	1.9	31	0.5	77	0.6	0.1
2002	186	365	360	1.5	374	1.5	32	0.6	79	0.8	0.0
2002	186	366	366	1.7	380	1.6	33	0.0	82	1.4	-0.1
2002	186	367	373	2.1	386	2.1	33	0.0	85	1.3	0.0
2002	186	368	381	2.2	394	2.2	33	0.0	87	1.0	0.0
2002	186	369	388	2.1	401	2.1	34	0.8	90	0.4	0.0

Relatively low OSD for both pyrheliometers are observed immediately before and after the minute (minute 361 = 06:01 UT) including the actual cleaning. This is indicative of a clear sky. The diffuse and global OSD are also low. At minute 361, the OSD for both pyrheliometers are abnormally high. This abnormality is also reflected in -6.4 (their difference, right column, shaded). The OSD for global and diffuse does not show any difference at that particular minute with respect to others.

The high OSD difference for pyrheliometers is put into perspective with Figure 3.14.

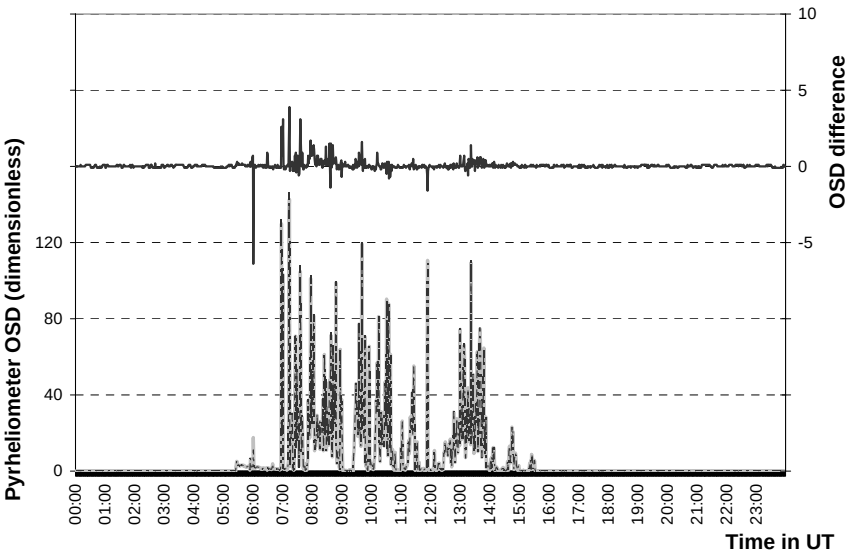

Figure 3.14 *Midnight-to-midnight time-series for 4 July 2002 of the shaded columns in table 3.4:* **(***Pyrheliometer A OSD (thick grey line) and pyrheliometer B OSD (dashed line) and difference (thin black line).*

Notice in Figure 3.14 that the outstanding number of -6.4 (at 06:01 UT) is by far the largest absolute difference between the pyrheliometers' OSD. This value, either positive or negative, never features elsewhere on that day, even though the OSD themselves reach high proportions as the day becomes partly cloudy from 07:00 UT onwards. Note that some differences in OSD are exhibited after 07:00 UT, but not to the extent of the -6.4 value.

To illustrate the conservativeness of pyrheliometer OSD difference with respect to individual pyrheliometer OSD fluctuations, consider Table 3.5. which depicts the same variables for the same day, 4 July 2002, but between minute 562 (09:22 UT) and minute 590 (09:50 UT).

Table 3.5 *One-minute De Aar data for 4 July 2002 between minutes 562 and 590.*

Year	Day of year	Minute of day	Pyrheliometer A		Pyrheliometer B		Diffuse pyranometer		Global pyranometer		Difference (N – M)
			AVG	OSD(M)	AVG	OSD(N)	AVG	OSD	AVG	OSD	
2002	186	562	782	0.5	793	0.3	132	2.2	584	2.6	-0.2
2002	186	563	782	0.1	794	0.2	140	2.6	593	2.7	0.1
2002	186	564	774	7.6	786	7.4	149	2.9	599	3.7	-0.2
2002	186	565	758	11.1	770	11.1	159	2.7	601	5.0	0.0
2002	186	566	663	22.4	675	22.5	168	3.2	557	14.4	0.1
2002	186	567	643	30.0	655	29.9	178	2.9	558	15.5	-0.1
2002	186	568	437	34.7	447	35.2	185	2.9	450	19.7	0.5
2002	186	569	554	45.9	566	46.3	195	2.1	529	27.8	0.4
2002	186	570	407	31.3	419	31.6	200	1.3	448	19.0	0.3
2002	186	571	506	36.6	518	36.5	206	2.0	512	22.5	-0.1
2002	186	572	575	22.9	587	23.1	212	1.5	556	14.2	0.2
2002	186	573	550	18.2	561	18.3	213	0.4	543	10.7	0.1
2002	186	574	571	32.1	581	32.1	212	1.8	554	19.5	0.0
2002	186	575	241	77.2	249	78.1	204	1.9	356	46.0	0.9
2002	186	576	185	19.8	192	20.4	202	0.7	322	12.4	0.6
2002	186	577	159	22.0	165	22.5	198	1.4	301	14.6	0.5
2002	186	578	146	14.4	152	14.7	192	1.7	288	8.0	0.3
2002	186	579	153	12.9	160	13.0	186	1.9	287	7.3	0.1
2002	186	580	237	55.4	245	55.9	180	2.0	331	32.9	0.5
2002	186	581	452	119.3	462	120.9	176	0.0	455	70.0	1.6
2002	186	582	545	21.6	557	21.8	170	3.3	502	15.1	0.2
2002	186	583	578	29.7	590	29.4	162	1.9	513	15.5	-0.3
2002	186	584	710	23.5	721	23.9	156	2.1	583	12.6	0.4
2002	186	585	691	17.6	703	17.5	148	2.1	566	10.7	-0.1
2002	186	586	629	42.5	641	42.9	141	2.5	523	27.3	0.4
2002	186	587	705	70.6	716	71.1	136	0.0	563	41.3	0.5
2002	186	588	765	4.8	776	4.7	134	1.3	594	1.9	-0.1
2002	186	589	777	2.4	788	2.4	129	1.3	598	1.5	0.0
2002	186	590	773	9.2	783	9.1	126	1.4	591	5.2	-0.1

Notice that high OSD for the individual pyrheliometers are not reflected in OSD difference close to the value of -6.4 featured in Table 3.4.

3.1.6 Aspects of the data acquisition system

Interaction between sensors and a data acquisition system may lead to a variety of errors experienced at De Aar, such as: runtime errors in the logger programme; wrong input signal measurement by logger due to ageing; overwriting of a data section in memory by program or vice versa; infrequent downloading leading to new data overwriting older data in logger and not enough room for error in case of power or computer failure, resulting in non-downloading of the logged data.

A good reliable and accurate datalogger forms the heart of any modern data acquisition system. It both measures and records sensor outputs as a basic function, while added value is the possibility of routine statistical calculations, such as the average, standard deviation, minimum and maximum of a number of samples on the data as they are collected. The latter proves to be a vital space saving mechanism when collecting data for the purpose of reporting the one-minute BSRN statistics. However, one disadvantage is, that the original samples are not available for re-evaulation should the need arise.

The ideal situation would be recording and storage of all measured samples, and applying calculations to produce the one-minute statistics only later on from the archived samples. An enormous logging and downloading capacity is a prerequisite, as well as a very reliable (ideally: dedicated) and short connection between the datalogger and site PC. This proved to be unfeasible for De Aar, given the large distance between the site at De Aar and SAWS Head Quarters in Pretoria, being 840 km apart. The best ecomonical logger byte-budget had to be compiled, to store as much information in the smallest space.

For typical data storage, note that one radiation parameter typically has 4 significant figures, therefore it needs a minimum of 5 digits to round the measured value off with confidence. One parameter therefore occupies 8 bytes of data (a space both sides, plus one for the decimal point). If every logged sample is date-and-time-stamped in the format *yyyy ddd hh mm ss* for future reference and/or recalculation it adds to a record containing 24 bytes, storing one sample per quantity. This is actually the area where a lot of space is still wasted, and, if resolved one way or the other, storing all the samples could be reconsidered.

In one minute, 60 samples are stored, 1440 bytes occupied per minute. For the basic quantities: global, direct and diffuse, the bytes amount to three times that amount. If LW measurements are also added to the same logger, three additional samples (thermopile, case and dome thermistors) are needed. This amounts to six times the said amount, 8640 per minute, or 12 441 600 bytes (11.86 MB) per day. This exceeds the logging capacity of a standard 1024 kb logger by almost 11½ times, neglecting room for a logging programme.

The raw data of 12 MB alone per day would fill the 10 GB hard drive, which was standard in a Personal Computer (PC) at that time, in less than 2 years leaving only little room for movement (backups or programs). Drastic economization steps had to be applied for De Aar, in order to create room for movement, whilst maintaining the highest possible resolution of data storage.

A very serious practical factor that had to be taken into consideration, was the distance of about 840 km between the site and headquarters. In the case of lightning strikes damaging the systems (three times between August 1999 and July 2003), enough room must exist on any given logger for data storage before a fresh PC can be dispatched to download the logger. This time lag is typically between 4 and 10 days.

The logging efforts were separated in a SW and a LW logger, each having unique characteristics and logging styles. This also doubled the logging capacity. In the case of a SW-logger, the samples can all can be processed in means, standard deviations, minima and maxima within the logger, without having to store 1 Hz samples. In the LW logger, recalculations warrant storage of original samples, whilst one-minute statistics of the measured components (thermopile, case and dome temperatures) cannot be applied to calculate the one-minute statistics of LWD. To store and date-time stamp all samples was not a feasible option, so a hybrid approach was followed. On the one hand, the logger program calculates LWD and reports one-minute statistics, but on the other hand, stores every n^{th} sample to have a number of samples per minute available for recalculations.

One sample in the new compact format looks like this :- *yyyy ddd hhmm dir1 dir2 dir3 dir4 dif1 dif2 dif3 dif4 glo1 glo2 glo3 glo4 lwd1 lwd2 lwd3 lwd4 temp hum pres* where yyyy = year, ddd = day of year (1 to 365 or 366), hhmm = time in hour and minute ; dir, dif, glo, lwd are the basic parameters direct, diffuse, global and downwelling longwave radiation, the number 1-4 behind these parameters are average, standard deviation, minimum and maximum, respectively; temperature, humidity, atmospheric pressure = meteorological quantities measured in a Stevenson screen. One record per minute in this new format, is 107 bytes long. This translates to 1.03 MB per week.

3.1.7 The usage of an on-site PC

A site PC is the “heart” of a data acquisition system, through its communication with a data logger. The PC compiles and sends a program to the logger and downloads data from the logger at preset intervals, it also stores and manages the downloaded data and communicates the data to the outside world, either by storage of data on removable media or transmission by means of network connections.

For De Aar BSRN, the multiple loggers demanded quasi-simultaneous processing in fast downloading of the relatively large volumes of data. This was achieved by a special serial port splitter, offering a unique serial port per device (logger). At the time of establishing the BSRN site at De Aar, modems and telephone connections were in the process of being phased out (Esterhuyse, 2000), and systems based upon a Wide Area Network (WAN) with PC terminals were the best outlook towards the future, and thus adopted.

3.1.8 Time keeping: Global Positioning System (GPS)

The high BSRN sampling frequency (1Hz) demands, that a high premium is placed on the correctness of time-stamping in sampled and derivated data products (one-minute statistics).

Time correctness is of further essence, since future research on data will involve the integration of datasets captured independently and under different circumstances and/or calculation of numbers, such as solar position, that involves accurate definitions of time. The biggest need for accuracy is when the sky is not clear, since small radiation features, which are the benefit of such high-resolution sampling, have to be correctly date- and time-stamped when captured.

At De Aar, the on-site PC is time-controlled by a Garmin GPS-36 polling a serial port once a second. The accurate PC time is transferred once every four hours to all system loggers and connected peripheral equipment.

3.2 MAINTENANCE SYSTEM

Due to the prolonged exposure of radiation instrumentation to solar radiation, regular maintenance is needed. This maintenance may consist of the following elements:

- Regular inspection (daily) of the general condition of the radiometers, including ventilation, levelling, pyrheliometer sun spots and shade spots. This also includes cleaning of all optical parts.

- Monthly inspection of the drying cartridges and electrical connections.

- Bi-annual (twice a year) calibration of the operational pyrheliometer, as well as swopping the global and diffuse pyranometers and turn-calibrate the pyranometers using the pyrheliometer calibration and the global/diffuse/direct relationship in Equation 3.5.

3.2.1 Regular inspection

A list of daily tasks comprises: Cleaning of instrument windows and domes, especially after precipitation events; Verification of tracker functions - reporting downtime. Verify, that all ventilators are functioning - and report downtimes. Inspection of solar spots on pyrheliometer and report misalignments.

3.2.2 Calibration

Regular calibration of SW radiation instruments, at least once a year, is recommended - six months being the normal proceedings (Mc Arthur, 1998). During a calibration event, the cavity radiometer is compared against the operational pyrheliometers. Conditions that have to be met, are the following:

- A cloudless day for periods when the global irradiance exceeds 700 $W.m^{-2}$
- No noticeable wind, as not to distort temperature stability in the cavity radiometer (WMO,1983).

The advantage of this *modus operandum* is that the pyrheliometers are not withdrawn from duty whilst in calibration mode. Their outputs are recorded with the cavity pyrheliometer's outputs, the ratios of (operational radiometer / cavity radiometer) are calculated for every period of integration (a "run") and new sensitivity constants are subsequently calculated for the pyrheliometers.

After the pyrheliometer constants are calculated, the global and diffuse pyranometers are swopped. The data of the periods before and after the swopping is used to determine new calibration constants for the pyranometers. In this way, the pyranometers are also out of operation for a short period of time, and if the swoppings are performed by night, no data at all need to be lost as a result of the calibration.

So far, only radiation measurement aspects have been discussed. A complete system comprises also management and communication of the recorded data.

3.3 DATA MANAGEMENT STRATEGY

A detailed plan on how data management is to be performed at sites, is featured in the work of Gligen *et al*. (1991). Some specific aspects, as realized at the De Aar site, are discussed in the following paragraphs.

3.3.1 On-site management

The outputs from the loggers should be visually displayed for easy inspection, identification and rapid rectification of typical operational bugs that might occur. Using a display system, frequent downloading from loggers leads to a minimum time lag and the displayed data is kept close to "real time". It also creates room for error, if systems are struck by lightning, they can be replaced with minimal data loss.

Another key element of the process is to keep individual file sizes manageable for easy handling afterwards, if only a small section of data (for example, a specific day) is required for any reason. One month of data of the SW and LW loggers combined, occupies 5 MB, which is difficult to handle (roughly 44000 records) if only one section of the data needed closer inspection. It was also difficult to handle by means of removable media of that time (a portable 3.5 inch disk holds about 1.44 MB). Bearing in mind that one day's data occupies the manageable size of about 160 kb per logger, daily files each assigned the date as a filename, was a logical choice. Memory-resident software truncates datafiles in midnight-to-midnight formats and assigns generic filenames to both LW and SW files. When preparing monthly submissions, the files for one particular month can be easily merged.

3.3.2 Management by station scientist

The main task of the station/site scientist is the supervision of BSRN data acquisition in terms of completeness and consistency (Hegner *et al*., 1998). In the process of doing so,

quality controls, assembly of files and preparation of data in the prescribed station-to-archive file format, are performed, using the dataflowstructure in Figure 3.15.

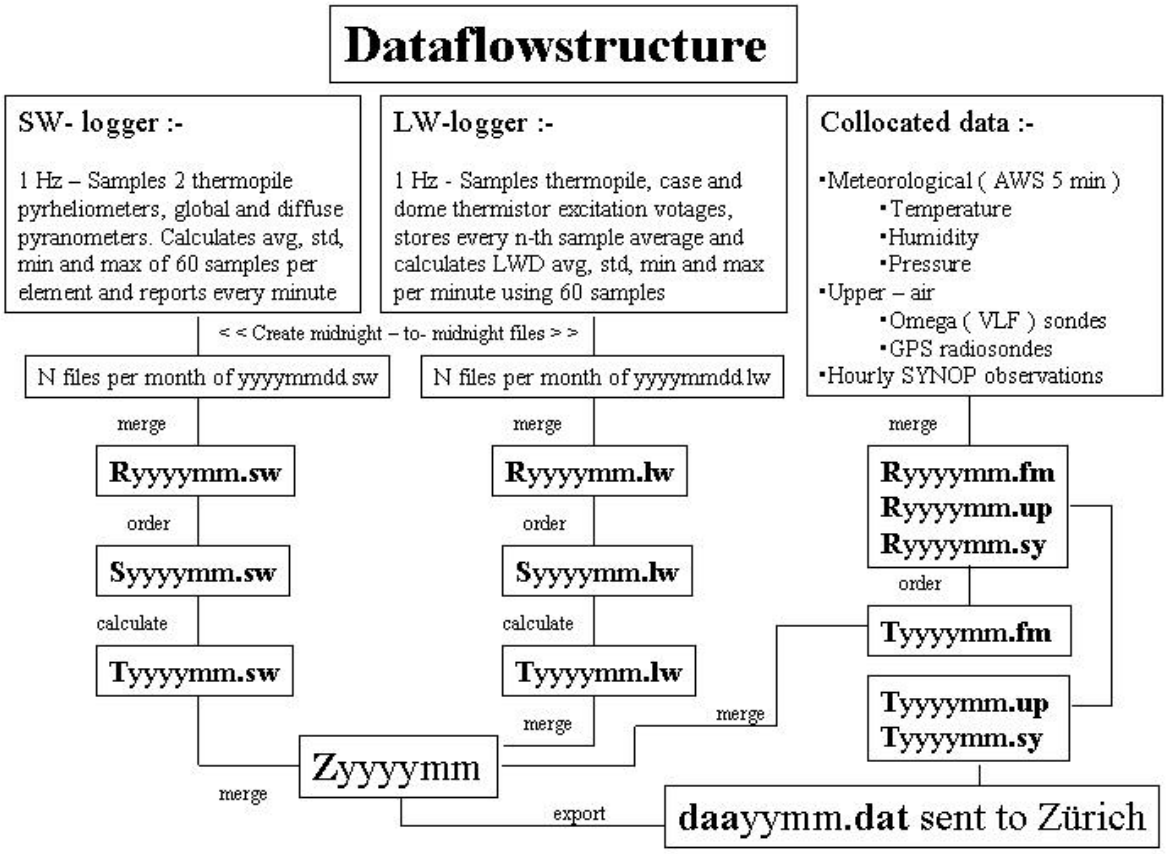

Figure 3.15 *Data management scheme for De Aar's data using generic filenames.*

The generic prefixes "R" (Raw), "S" (Sorted) and "T" (Final) each indicate different levels of refinement. A higher level of refinement is reached by running a tailor-made application developed in Fortan and run on the SAWS main-frame computers.

3.4 LIAISING WITH INTERNATIONAL DATABASE

During the Davos 1991 meeting (WCRP-64) it was decided to have all the BSRN data located at and managed by a central database, located at WRMC, ETHZ in Zürich, Switzerland. At the same institution (ETHZ), the database of GEBA is also maintained, and it follows naturally that the BSRN database was developed in the GEBA style.

3.4.1 The GEBA database

A short description of the GEBA database and relevant overlaps with the current BSRN database, to put them into perspective, is presented.

The GEBA was implemented in 1988 as a project of the Global Climate Program: Water and is a database of conventional surface radiation fluxes measured at approximately 1500 sites globally, in monthly mean values only, starting with data collected in the late 1940's up to present. A redesign of the database took place in 1994, which enabled removal of contradictions, updating of data and improving the quality control procedures for global radiation (Gilgen *et al*., 1998) but the basic format remained.

Although upward and downward flux densities of both solar and terrestrial radiation measurements appear in the database, the best represented parameter by far (87%) is global radiation, as measured with an upwardly facing horizontally mounted pyranometer according to the latest update (Gilgen and Ohmura, 1999). Extra value is added to the data by means of an extensive accompanying metadata file containing accurate descriptions of instrument types, units and varying degrees of compliance to the different pyrheliometric scales (Angstrom, IPS, WRR) that were phased in as these datasets were being recorded.

For quality control procedures, compliance of all data using the following procedures, each defined by physical properties founded in theoretical, as well as empirical quantities, are applied to the GEBA data (Gilgen *et al.*, 1997)

- The testing of "Physically possible" boundaries – i.e., the compliance of the data to numbers determined by physical constraints;
- The testing for "Physically probable" boundaries – i.e., a more strict test, identifying questionable data that passed the previous test;
- The compliance of global radiation data to a parameterized value, using total cloud amount;
- The compliance of standard deviations of a time series of yearly means for a data set, to predetermined boundaries;

- The compliance of a difference time series of yearly means, to predetermined values;

- Quantifying the conforming to a norm of differences that might exist in monthly climatologies, using long-term datasets.

The procedures were designed in order of increasing intricacy – i.e., a data value not passing procedure n, is very unlikely to pass procedure n+1, etc. Addition of quality control flags to all the data as a data point passes or fails a specific procedure is done the same way as for the BSRN database. The BSRN have different methodologies to test data boundaries, described and investigated in Chapter 4.

The synchronization of data collected in different time zones is not necessary, since the integration time for data is larger than one day (only monthly averages are used in GEBA). In the BSRN case, all data is recorded in UT to allow direct intercomparison, for any reason, of quantities taken in different time zones of the world.

3.4.2 The BSRN database

The WRMC, responsible for managing the BSRN database, is run by the Division of Climate Sciences at the Institute of Geography, ETHZ, Switzerland. Its main tasks towards the BSRN community are defined (WCRP-54, 1991) as: Receive data from the BSRN sites and, if the data fulfill the consistency requirements, insert them into the BSRN database; Check the quality of the radiation data and add quality control information to each radiation value in the BSRN database (quality check flags); Report doubtful values to BSRN stations and respond to queries; Update, maintain and safeguard the BSRN database; Combine the data from different sites, calculate and store statistics; Redistribute the data; Submit an annual report to the BSRN Science Review Panel; and distribute annual data approved by the review panel to the BSRN stations and external persons.

The database is therefore designed to play a very important supportive role in the ongoing functioning of the network, and in this respect, the maintaining of sound relationships with all the member sites, is vital.

A typical communication episode between the site scientist and database manager concerning a data file would be as follows:

- Archiving and compilation of one logical unit (month) of data under supervision of site scientist.

- Submitting of the monthly file, following the exact station-to-archive file format (details in Appendix B).

- Database manager runs basic programmes to check for data line lengths, the possibility of unacceptable characters and ambiguousities, and file consistency.

- If inconsistencies are found, the station scientist is notified and corrections are made. A corrected version of the data is submitted. The site scientist is the only person allowed to change data.

- The data quality is controlled, and feedback in the form of a monthly report is given to the site scientist.

- This process is repeated until the two parties agree to settle.

Data quality flags are added in the data stored at the BSRN database, but the flags are not included in data provided to outside parties. The station scientist is the only person in a correct position to change data, since he/she has access to the original data and observational procedures, and can hence be in the best position to identify erroneous values (Gilgen *et al.*, 1997).

3.5 CONCLUSION

In a radiation measuring system, the integration and management of components is vital in smooth functioning of the system. Staying abreast with new technology is an important step in maintaining its relevance. In the same way that frequent physical inspection of the instruments reveals operational errors that must be kept to a minimum, frequent reflection on the relevance of the entire measurements reveals shortcomings that can be rectified so that the system justifies its existence and serves its original purpose.